Nuclear Engineering and Technology 52 (2020) 1517–1523

Contents lists available at ScienceDirect

Nuclear Engineering and Technology

journal homepage: www.elsevier.com/locate/net

Original Article

Development of fission ^{99}Mo production process using HANARO

Seung-Kon Lee [a, *], Suseung Lee [a], Myunggoo Kang [a], Kyungseok Woo [a], Seong Woo Yang [a], Junsig Lee [b]

[a] Neutron and Radioisotope Application Research Division, Korea Atomic Energy Research Institute, 111 Daedoek-daero 989beongil, Yuseong-gu, Daejeon, 34057, Republic of Korea
[b] Korea Multi-purpose Accelerator Complex, Korea Atomic Energy Research Institute, 181 Mirae-ro, Geoncheon-eup, Gyeongju-si, Gyeongsangbuk-do, 38180, Republic of Korea

ARTICLE INFO

Article history:
Received 30 September 2019
Received in revised form
16 December 2019
Accepted 17 December 2019
Available online 20 December 2019

Keywords:
Molybednum-99 (Mo-99)
Low enriched uranium
Medical radioisotope
Technetium-99 m (Tc-99 m)
Research reactor

ABSTRACT

The widely used medical isotope technetium-99 m (^{99m}Tc) is a daughter of Molybdenum-99 (^{99}Mo), which is mainly produced using dedicated research reactors from the nuclear fission of uranium-235 (^{235}U). ^{99m}Tc has been used for several decades, which covers about 80% of the all the nuclear diagnostics procedures.

Recently, the instability of the supply has become an important topic throughout the international radioisotope communities. The aging of major ^{99}Mo production reactors has also caused frequent shutdowns. It has triggered movements to establish new research reactors for ^{99}Mo production, as well as the development of various ^{99}Mo production technologies. In this context, a new research reactor project was launched in 2012 in Korea.

At the same time, the development of fission-based ^{99}Mo production process was initiated by Korea Atomic Energy Research Institute (KAERI) in 2012 in order to be implemented by the new research reactor. The KAERI process is based on the caustic dissolution of plate-type LEU (low enriched uranium) dispersion targets, followed by the separation and purification using a series of columns. The development of proper waste treatment technologies for the gaseous, liquid, and solid radioactive wastes also took place. The first stage of this process development was completed in 2018. In this paper, the results of the hot test production of fission ^{99}Mo using HANARO, KAERI's 30 MW research reactor, was described.

1. Introduction

Since the discovery of molybdenum-99 (^{99}Mo, $T_{1/2}$ = 2.75 d) generator technology in the 1960s by Walt Tucker and his colleagues in Brookhaven National Laboratory, the radioisotope has been one of the most important medical radioisotopes in the last 60 years [1–4]. It is due to the technetium-99 m (^{99m}Tc, $T_{1/2}$ = 66 h), the daughter of ^{99}Mo, which has become popular as a diagnostic nuclear medicine because of its excellent nuclear properties. The 140.5 keV gamma emission from ^{99m}Tc is equivalent to the X-ray, which typically ranges from 20 to 150 keV, and is ideal for gamma imaging such as SPECT. Its short half-life is also suitable as a medical tracer [5,6]. Although ^{99m}Tc was discovered in the 1930s, the availability of the radioisotope was limited until the 1960s due to its short half-life, as well as the absence of corresponding labeling compounds [7,8].

With the radioisotope generator technology, the single supply of longer-lived parent, ^{99}Mo, facilitates the utilization of its daughter, ^{99m}Tc, in the hospital for about two weeks. For generator applications, the radioactive equilibrium of the parent and daughter nuclides is mandatory. The half-life of ^{99}Mo is longer than its daughter, and the balance between their radioactive decay and growth converges into a transient equilibrium [2–4].

On the other hand, the development of various cold kits containing ligands to form complexes with ^{99m}Tc widened its diagnostic applications to various diseases such as bone scans, myocardial perfusion imaging, cardiac ventriculography, brain imaging, and blood pool labeling. There are currently more than 100 cold kits approved by the Food and Drug Administration (FDA) of the United States. These include DTPA, MDP, DMSA, and MIBI [7,8]. As a nuclear medicine, this radionuclide has now become the most commonly used radioisotope, as it covers more than 80% of overall diagnostic procedures in the world including tens of millions

* Corresponding author.
E-mail address: seungkonlee@kaeri.re.kr (S.-K. Lee).

https://doi.org/10.1016/j.net.2019.12.019

procedures annually [4,9].

The worldwide market for ^{99}Mo/^{99m}Tc has been mainly covered by demands from United States and Europe, but recently, demand is growing in Asian and African markets. However, the aging of major ^{99}Mo producing reactors has been caused by an unstable supply such as the ^{99}Mo crisis in 2009. The aforementioned situation stimulated international cooperation through the IAEA and the OECD-NEA for the stable supply of ^{99}Mo [4,9]. It also promoted the construction of new research reactors in other countries, as well as the development of various ^{99}Mo production technologies other than fission: The neutron capture and accelerator-based ^{99}Mo production. ^{99}Mo can be produced by the neutron capture reaction: ^{98}Mo (n, γ) ^{99}Mo. The neutron capture production scheme has advantages in simple chemical process and suppressed radiowaste generation. However, the ^{98}Mo neutron capture gives low production yield due to the small neutron absorption cross-section of the ^{98}Mo from the natural Mo (thermal neutron cross-section, $\sigma_{th} = 0.14$ b), in comparison with the ^{235}U thermal fission cross-section ($\sigma_{th} = 584$ b) As a result, the specific activity of ^{99}Mo produced using fission is 2500–10,000 times higher than the ^{99}Mo produced using the neutron capture (1–4 Ci/g).

Recently, production of ^{99}Mo from ^{100}Mo target using the ^{100}Mo (γ, n) ^{99}Mo reaction or ^{100}Mo (n, 2n) ^{99}Mo reaction is being investigated. SHINE Medical Technologies is constructing the fission ^{99}Mo production facility based on the bombardment of accelerator produced neutron onto the liquid uranium target. However, it will take more years for the commercial-scale production of the ^{99}Mo using accelerators.

Because of the aforementioned reasons, over 90% of the ^{99}Mo supply depends on the fission ^{99}Mo, which has been proven for few decades with their large-scale productivity and high specific activity (~10^4 Ci/g) [10–16].

In the same context, the first stage of the fission-based ^{99}Mo production technology development for a new research reactor in Korea was carried out by KAERI during 2012–2018. The ^{99}Mo production technology was designed for the reactor-based fission ^{99}Mo process that uses low enriched uranium (LEU) targets [17]. In this study, the results of the hot test production for the fission ^{99}Mo process development from depleted uranium (DU) targets irradiated in HANARO, KAERI's 30 MW research reactor, was described.

2. Methods

2.1. Process scheme for the hot test production in HANARO

The production of the ^{99}Mo starts from irradiating the uranium target in the research reactor. Plate-type dispersion targets with uranium aluminide (UAlx) meat are assembled in capsules and a rig for irradiation in HANARO. After the irradiation, the target is transferred to the hot cell located at KAERI's Irradiated Materials Examination Facility by using a transport cask. In the IMEF hot cell, a crude ^{99}Mo solution is produced through a dissolution process, uranium filtration, iodine removal, and off-gas treatment. The crude ^{99}Mo solution is then further separated from the other impurities and fission products. The samples in this study were collected from each process step for analysis. Fig. 1 shows the flow of fission-based ^{99}Mo production.

2.2. Uranium target and irradiation test

Plate-type dispersion targets with uranium aluminide (UAlx) meat and aluminum alloy cladding were fabricated by KAERI. The uranium powder was prepared using the signature technology of KAERI: Centrifugal atomization [18]. LEU and DU targets were prepared for different purposes, respectively. LEU targets were made to verify the target itself through an irradiation test and post irradiation examinations.

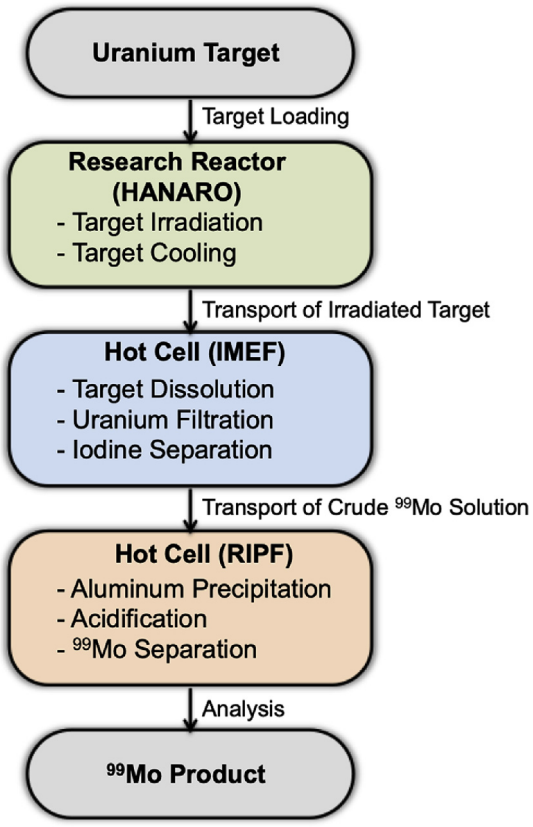

Fig. 1. Schematic process flow of fission-based ^{99}Mo production in HANARO.

Recently, major ^{99}Mo producers have converted their highly enriched uranium (HEU) targets to a low enriched uranium (LEU) target for nuclear non-proliferation, as supported by the related international societies [19–22]. KAERI also developed a LEU-based ^{99}Mo production technology for compliance with international policy. DU targets were produced for the hot test production of ^{99}Mo at HANARO. Irradiation capsules and a rig for the DU targets were designed and fabricated for the hot experiments. The DU plate targets were assembled with irradiation capsules made of aluminum alloy and then inserted into the rig under HANARO's working pool. The DU target rig assembly was then transferred to a reactor pool, where the reactor core is located. The rig containing two uranium target capsules was loaded into an out-core hole (IP6) for irradiation during the 97th period of HANARO operation. After irradiation for two days, the targets were cooled down for two additional days. Finally, the irradiated DU targets were transported to the hot cell in the IMEF by using a fuel cask and truck. Fig. 2 shows the overall procedures of target irradiation and transport.

2.3. Dissolution of uranium target

^{99}Mo can be obtained from the neutron-irradiated uranium targets through a certain series of chemical processes. The entire ^{99}Mo production process can be systematically integrated and carried out sequentially, batch by batch [23–25].

The ^{99}Mo production system demonstrated in this paper was made of two separate systems. A system for the target dissolution process, including the handling of nuclear materials, was installed and operated in an IMEF hot cell. The main purpose of the target dissolution system is to dissolve the neutron-irradiated uranium

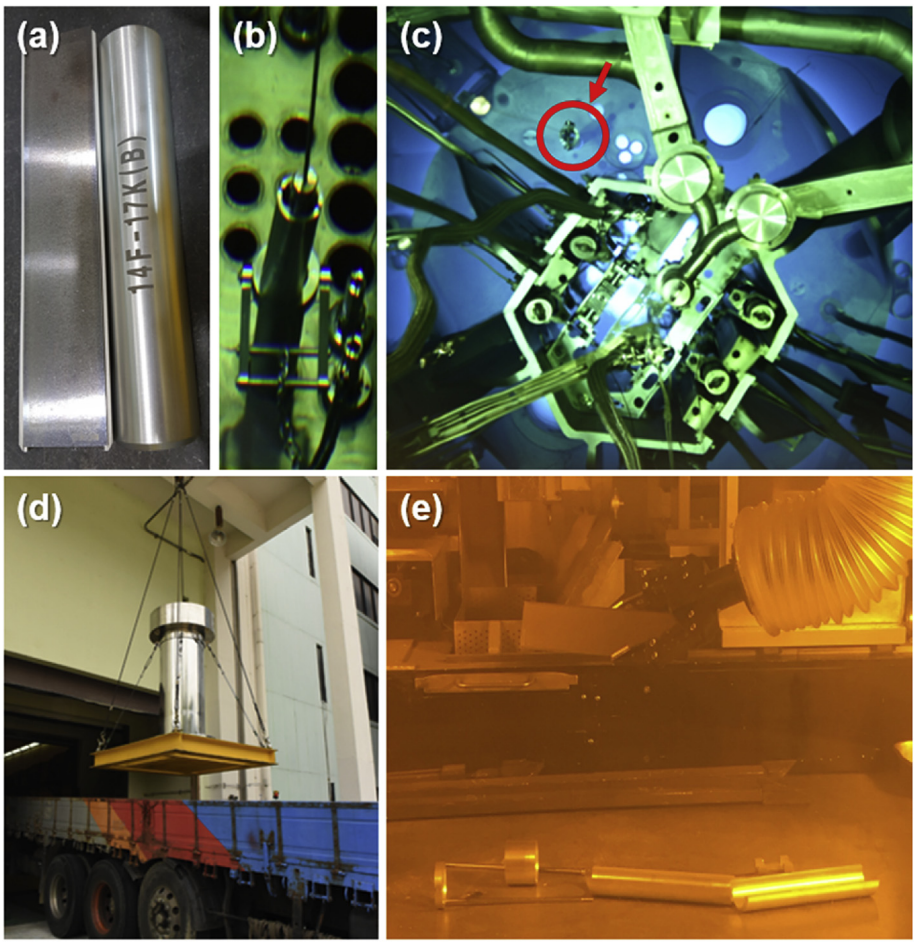

Fig. 2. Flow of target irradiation and transport in HANARO facilities. (a) Target and irradiation capsule. (b) Loading DU target capsule into the irradiation rig under the HANARO working pool. (c) Irradiation of the target rig assembly in the IP6 (red circle) of HANARO. (d) Transport of the irradiated target capsule from HANARO to IMEF using a fuel cask. (e) Disassembly of the target capsule for the dissolution process in the IMEF hot cell. (For interpretation of the references to colour in this figure legend, the reader is referred to the Web version of this article.)

target to eliminate the uranium/transuranic compounds, aqueous radioiodine species, and radioactive gases from the ^{99}Mo production stream. Fig. 3 shows the dissolution system designed to treat the single DU plate target with the following steps.

The dissolver is a jacketed reaction vessel that has a lid for the target loading. The chemical reactants can be transferred and loaded from outside the hot cell through the pre-installed supply tubes. The temperature of the system can be controlled from the equilibrium between an electric coil heater and cooling jacket. The water-cooled reflux condenser is located on top of the dissolver vessel to collect the vaporized solution from the off-gas stream during high-temperature reactions [23–25].

A filter unit was mounted directly under the dissolver to separate the unreacted uranium compounds and other precipitating elements, including transuranic nuclides. A sintered metal powder filter (STS-316L) with 3.2 mm thickness was used as a filter media. The filter unit was designed to easily replace hot cells that use master-slave manipulators [23–25].

Cylindrical columns packed with home-made silver-doped alumina were used to trap and remove the aqueous radioiodine species from the digestion solution [26]. The required quantity of adsorbents was estimated conservatively to ensure the complete elimination of the radioiodine species. A solution transfer was performed with a constant flow rate using a peristaltic pump.

The hydrogen generated from the caustic dissolution of the target was eliminated using the catalytic converter. The hydrogen converter is a cylindrical column packed with copper oxide rods that have a uniform diameter and a length of 3–4 mm. An electric coil heater and PID controller were equipped to control the column temperature up to over 400 °C. Hydrogen gas oxidized into water vapor on the surface of the copper oxide materials [27].

A cylindrical tank with 70 L volume was installed in the hot cell and connected to the dissolving system. Its primary function is to collect and store all process off-gas from the system. Various gaseous radioisotopes with radioactive noble gases and radiohalides are required to be trapped for safety [28]. In addition, the vessel pressure of the dissolver and reservoir can be adjusted so that the induced pressure difference can be utilized between two vessels.

On the other hand, the pressure of production vessels was controlled using the vacuum tank. The pressure displacement between two neighboring vessels is a driving force to transfer process liquid or reactant from one vessel to another.

All of the above-mentioned process units were made with stainless steel and assembled on the aluminum support, as shown in Fig. 4. Finally, the integrated dissolving system was installed in an IMEF hot cell for hot demonstration. The airtightness of the entire system with multiple vessels, tubing, valves, and connections were tested and confirmed prior to the experiment. The product from the dissolving process is the crude ^{99}Mo solution, which contains a

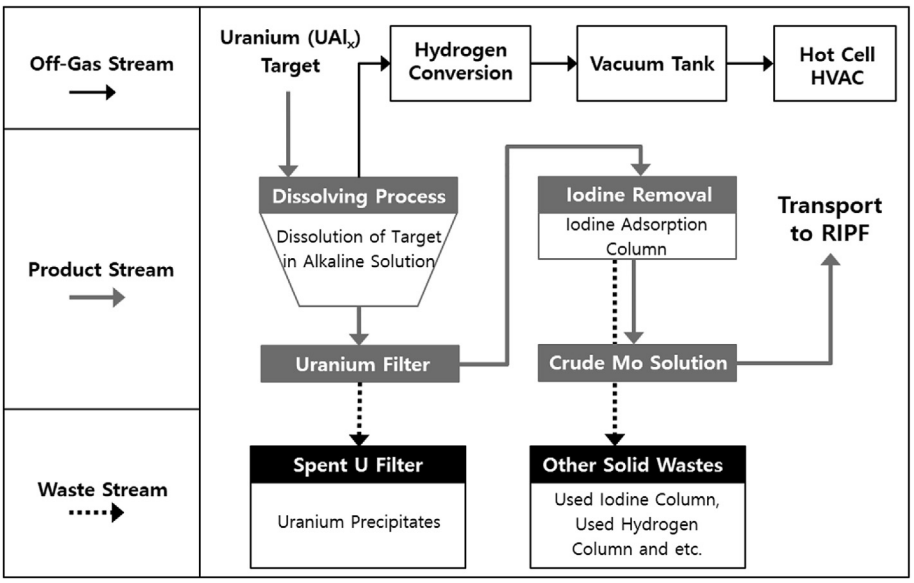

Fig. 3. Process flow diagram of the target dissolution processes designed for the hot test production. The solid grey line shows the main stream of the ^{99}Mo flow. The dotted black line shows the solid waste stream. The solid black line represents the off-gas stream.

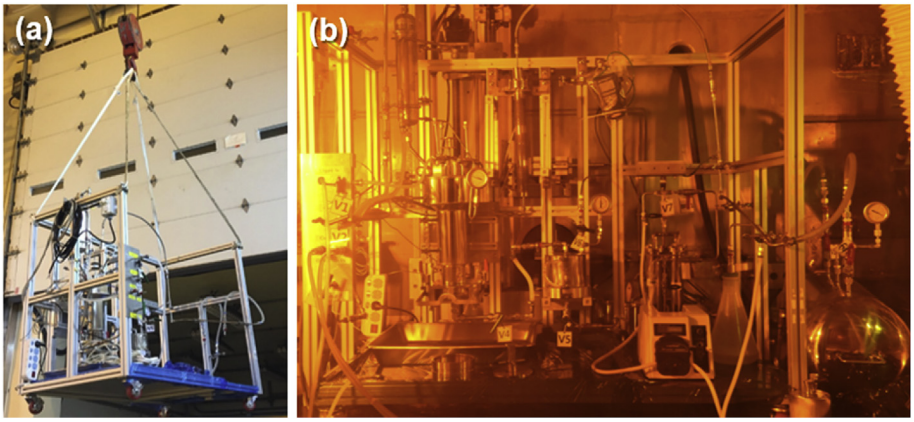

Fig. 4. Target dissolution system constructed for the hot demonstration. (a) Installation of the dissolution system using a crane. (b) Dissolution system installed in an IMEF hot cell.

majority of ^{99}Mo and water soluble elements.

2.4. ^{99}Mo separation process

The system for the ^{99}Mo separation process without any nuclear materials was installed and operated in an RIPF hot cell. Fig. 5 presents the scheme for the ^{99}Mo separation system with process equipment. The ^{99}Mo separation system consists of a precipitation vessel, filter cage, acidification vessel, and separation column. Fig. 6 shows the ^{99}Mo separation system installed in the RIPF hot cell.

Practically, the quantity of the total ^{99}Mo presence in the target solution is tiny (~0.1% of the total fission products). The most important chemical compound in the crude ^{99}Mo solution is the dissolved aluminum, which forms $Al(OH)_3^-$ under an alkaline solution.

In the precipitation vessel, dissolved aluminates were removed by a precipitation reaction. Herein, the aluminum ion was transferred to aluminum hydroxide ($Al(OH)_4^- \rightarrow Al(OH)_3(s)\downarrow + OH^-$) under a pH 9–10. As a pH buffer, CO_2 gas was introduced in the precipitation vessel to control the solution pH. When the CO_2 gas dissolved in water, it forms a carbonic acid ($CO_2(g) + H_2O \leftrightarrow H_2CO_3$). In addition, the carbonic acid neutralizes the solution's alkalinity. A filter cage is needed to remove the aluminum precipitates from the solution in the precipitation vessel.

The conditioning of the ^{99}Mo containing solution was carried out in the acidification vessel, prior to the column separation. A separation column with a chelating ion exchange resin was used to increase the ^{99}Mo separation efficiency under an acidic condition. Also, the ^{99}Mo ions in the solution should have a Mo-thiocyanate complex compound to increase the residence time in the separation column. Finally, the separation column filled by the chelating ion exchange resin selectively adsorbs the modified ^{99}Mo in the acidified solution.

Samples from the final ^{99}Mo solution were taken for the further analysis. Based on the impurity levels in the solution, a further purification step may be needed.

3. Results and discussion

3.1. Target dissolution and iodine separation

An irradiated target capsule was transferred from HANARO to

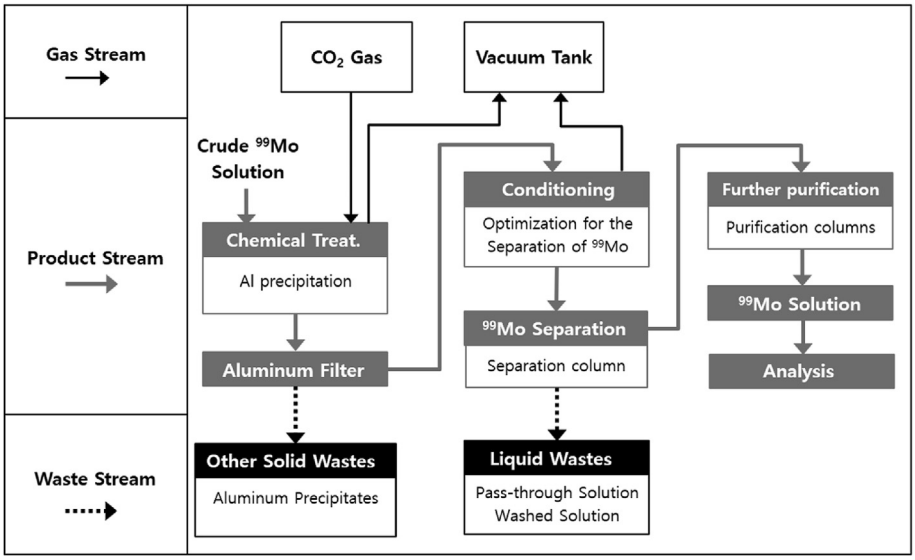

Fig. 5. Scheme for the ^{99}Mo separation system designed by KAERI. The solid grey line shows the main stream of the ^{99}Mo flow. The dotted black line shows the solid and liquid waste streams. The solid black line represents the gas and vacuum streams.

Fig. 6. ^{99}Mo separation system installed in an RIPF hot cell.

the hot cell in IMEF using a fuel cask. The target capsule was then carefully disassembled using manipulators equipped with dedicated tools.

The DU target plate taken from the capsule was inserted to the dissolver filled with 3 M sodium hydroxide (NaOH) solution. The reaction was triggered as we increased the solution temperature to above 60 °C. Aluminum and uranium species in the target plate reacted with sodium hydroxide to produce sodium aluminate ($NaAlO_2$) and a few kinds of uranium compounds, mostly uranium oxide (UO_2) and sodium diuranate ($Na_2U_2O_7$) forms [25]. Although the reaction between aluminum and sodium hydroxide is highly exothermic, additional external heat was added through an electric coil heater to promote the initial reaction rate (Equation (1)). The temperature of the solution was kept constant at about 80 °C throughout the process.

$$2Al + 2NaOH + 2H_2O \rightarrow 2NaAlO_2 + 3H_2 (\text{exothermic reaction}) \quad (1)$$

The internal pressure of the dissolver was also maintained at a steady pace with a negative pressure condition near −0.05 MPa in order to prevent the leakage of process off-gas. In addition, the system pressure was controlled by adjusting the valve linked to the vacuum tank. The hydrogen converter located between the dissolver and vacuum tank operated under a very high temperature over 350 °C during the target dissolution process. This eliminated the hydrogen gas from the off-gas stream by converting it into water vapor (equation (2)) [27]. The final destination for the off-gas stream without hydrogen was the vacuum tank.

$$CuO + H_2 \rightarrow Cu^0 + H_2O \quad (2)$$

With the vigorous caustic dissolution reaction for over 70 min, the DU target plate completely collapsed and was digested in the solution. Multiple water-soluble fission products, including the ^{99}Mo, were eluted into the solution as cationic or anionic forms. The digestion solution also contained colloidal suspensions from the precipitation of insoluble compounds. The precipitates can be removed by filtration using a sintered metal powder filter. In particular, most of the unburned uranium compounds and trans-uranic species were collected from the filter media and were completely segregated from the ^{99}Mo containing solution stream.

The filtered solution then passed through the iodine column to remove the radioiodine species from the solution. The iodine removal columns were filled with the alumina particles doped with silver nanoparticles, which showed a high radioiodine removal efficiency (99.7%) from the previous studies [2]. The final ^{99}Mo containing solution was sampled and analyzed with a HPGe gamma spectrometer. No significant radioiodine species was identified through the analysis. The crude ^{99}Mo solution from the target dissolution system was collected and sealed in the stainless-steel bottle. The bottle was then transported to the hot cell in RIPF for the subsequent ^{99}Mo separation process, using a cask originally designed for the Ir-192 transport.

3.2. ^{99}Mo separation

Crude ^{99}Mo was introduced to the ^{99}Mo separation system installed in the RIPF of KAERI. To minimize the potential release of volatile radioactive species, the separation system was operated

under weak a vacuum condition as a closed system.

The crude ^{99}Mo bottle was connected to the precipitation vessel in the separation system (Fig. 1). The solution in the bottle was transferred by a vacuum suction. Then CO_2 gas was injected to the vessel to initiate aluminum precipitation. As the aluminum precipitation reaction proceeded, the solution became translucent in the beginning, and opaque later on. The turbidity of the solution was due to the generation of aluminum hydroxide colloidal particles. After precipitation, the $CaCl_2$ solution was added in the vessel to remove excess carbonate ions ($Ca^{2+} + CO_3^{2-} \rightarrow CaCO_3(s)\downarrow$, $K_{sp} = 1.4 \times 10^{-8}$). The precipitates containing $Al(OH)_3$ and $CaCO_3$ were removed by using a filter cage. The filter cage was gently washed with deionized water to minimize the loss of the co-precipitated ^{99}Mo species. The filtrates and washed solution were collected together in the acidification vessel. Ascorbic acid and KSCN were added into the acidification vessel to synthesize the Mo-thiocyanate complex. H_2SO_4 was dropped in the vessel to decompose any remaining carbonate ions, which affect the efficiency of the separation yield. After conditioning in the acidification vessel, the ^{99}Mo containing solution passed through the column filled with the chelating ion exchange resin to adsorb the ^{99}Mo complex. Finally, the ^{99}Mo collected in the column can be eluted from the separation column using a 1 M NaOH solution.

3.3. Calculation of nuclear reaction

The production of various nuclides through the nuclear fission was calculated by using the burnup calculation module of MCNP6 and ORIGEN 2.2. Each calculation utilized the ORIGEN library data produced from the nuclear data and neutron flux at the exact irradiation location. Both calculations showed almost identical results with about 1% difference. The estimated ^{99}Mo activity calculated with MCNP6 ranged from 2.180 to 2.41 Ci, and the value acquired from the ORIGEN 2.2 ranged from 2.157 to 2.388 Ci, respectively. The average power generation from a single DU target ranged from 111.90 to 123.97 W, which fulfilled the operation conditions needed to run HANARO safely.

3.4. Analysis

To trace the flow of ^{99}Mo species during the separation process, the samples were collected at each step: The crude ^{99}Mo solution (sample 1), the filtrates after aluminum precipitation (sample 2), the eluted ^{99}Mo solution from the separation column (sample 3), and the effluent of the separation column, which represents the waste stream (sample 4). The presence of the radionuclides in the samples were determined by using a HPGe gamma-ray spectroscopy [25]. Fig. 7 shows the gamma spectra taken from the samples.

The quantitative analysis was carried out using the 739.5 keV peak, which has highest efficiency among the ^{99}Mo gamma spectra. The calibrated activity of the crude ^{99}Mo solution (sample 1) was 681 mCi, which corresponds to 34% of the predicted inventory calculated in section 3. 3. The separation yield (120.8%) of the ^{99}Mo was measured by comparing the activities of the filtrates after aluminum precipitation (sample 2, 24 mCi) and the eluted from the separation column (sample 3, 29 mCi). The overall recovery yield can be calculated by comparing the activities of the crude ^{99}Mo solution (sample 1) and the eluted ^{99}Mo solution from the separation column (sample 3). The overall recovery rate was 4.3%, due to the co-precipitation of the ^{99}Mo in the aluminum precipitation step. Although the KAERI's unique aluminum precipitation process, prior to the ^{99}Mo separation, has several advantages, such as simplified purification process and easy treatment of the intermediate level liquid waste stream, the majority of ^{99}Mo remain in the aluminum precipitates. The recovery yield could be enhanced by adding the eluted ^{99}Mo from the aluminum precipitates.

No peaks associated with ^{131}I (284.3 keV 6.06%, 364.5 keV 81.22%, and 637.0 keV 7.27%) were observed from the samples. This result representing no iodine species existed in the solution, and the peaks were successfully removed from the dissolving system through the iodine removal column.

^{99}Mo peaks from the gamma spectra of samples 1, 2, and 3 verified the presence of ^{99}Mo throughout the entire separation process flow. This meant there was a successful connection of each process step in the separation system. Not only ^{99}Mo (181.1 keV 6.07%, 366.4 keV 1.16%, 739.5 keV 12.14%, and 777.9 keV 4.35%), but

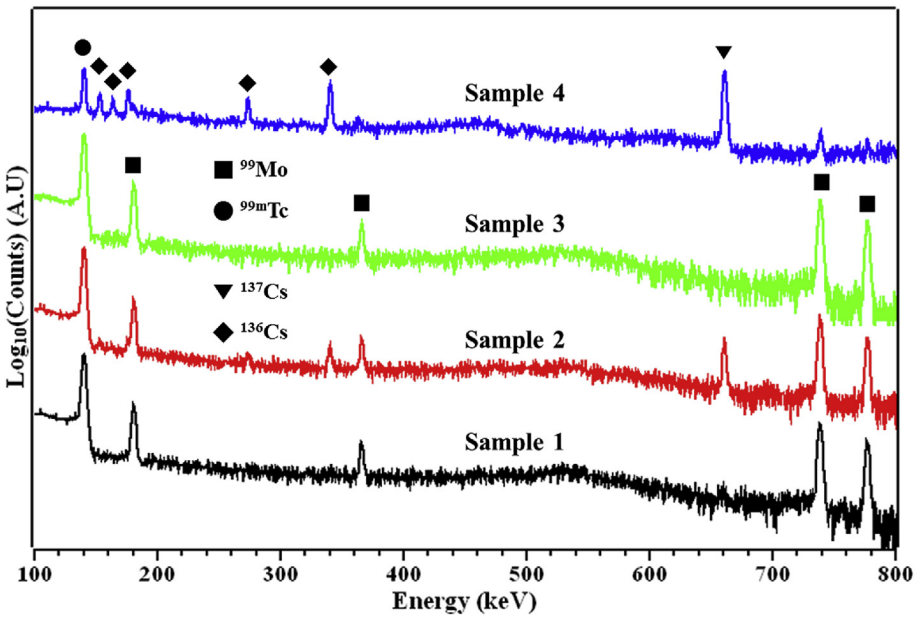

Fig. 7. Gamma spectra of samples collected at each step. The crude ^{99}Mo solution (sample 1), the filtrates after aluminum precipitation (sample 2), the eluted ^{99}Mo solution from the separation column (sample 3), and the effluent of the separation column (sample 4).

also the other fission products such as ^{99m}Tc (140.5 keV 87.2%), ^{136}Cs (153.3 keV 7.47%, 164.0 keV 4.62%, 176.6 keV 13.63%, 273.7 keV 12.69% and 340.6 keV 48.61%), and ^{137}Cs (661.7 keV 85.21%) were analyzed from the gamma spectrum of the filtrates sampled after the aluminum precipitation process.

The ^{99}Mo solution sample taken from the elutes of the separation column presented only ^{99}Mo and ^{99m}Tc, which were generated by the decay of ^{99}Mo. These results strongly support the successful separation of ^{99}Mo species from the dissolution of the irradiated uranium target and also from the following separation process.

On the other hand, the effluent from the separation column, representing the liquid waste stream, mainly showed peaks from other fission products. This confirms that a tiny fraction of ^{99}Mo flow was in the waste stream as a loss. In addition, the majority of the produced ^{99}Mo exists in the separation column.

4. Summary

^{99}Mo has long been one of the most important isotopes as a parent of the most commonly used medical isotope, ^{99m}Tc, for diagnosis. In this study, the overall ^{99}Mo production scheme was presented. In particular, the fission-based ^{99}Mo production process developed by KAERI was described, with their recent hot demonstration using HANARO in 2018. The DU plate-type targets were fabricated for the test and irradiated in HANARO for about two days, which resulted in ^{99}Mo generation with other fission products. The development was verified by sample analysis with gamma spectroscopy.

The results of the development presented in this study are the first steps toward commercial-scale ^{99}Mo production. Further development of the mass production technology is required for the practical implementation of the process to other Korean new research reactors as a second stage development. In the future, quantitative analysis will be added for more accurate quality control. On the other hand, an effective strategy to reduce the waste generation from the fission ^{99}Mo production will become more important. This is because a dramatic increase in the intermediate level liquid waste is expected from the conversion of LEU targets instead of the HEU in the ^{99}Mo production [29]. The final goal of the project is to aim for the weekly production of 2000 Ci (6-day calibrated) ^{99}Mo from the new research reactor, which corresponds to 100% of domestic demand, as well as about 20% of the international market.

Declaration of competing interest

The authors declare that they have no known competing financial interests or personal relationships that could have appeared to influence the work reported in this paper.

Acknowledgements

This work was supported by the National Research Foundation of Korea (NRF), funded by the Ministry of Science and ICT (NRF-2017M2A2A6A01071321 and NRF-2017M2A2A6A05016598).

References

[1] International Atomic Energy Agency, Production Technologies for ^{99}Mo and ^{99m}Tc, IAEA-TECDOC-1065, IAEA, Vienna, 1999.
[2] International Atomic Energy Agency, Non-HEU Production Technologies for Molybdenum-99 and Technetium-99m, IAEA Nuclear Energy Series, No. NF-T-5.4, IAEA, Vienna, 2013.
[3] National Research Council of the National Academy of Sciences, Medical Isotope Production without Highly Enriched Uranium, National Academic Press, Washington D. C., 2009.
[4] L.G. Stang, Manual of Isotope Production Processes in Use at Brookhaven National Laboratory, BNL-864, Brookhaven National Laboratory, Upton, New York, 1964.
[5] H. Anger, A New Instrument for Mapping Gamma-Ray Emitters. Biology and Medicine Quarterly Report, UCRL-3653, University of California Radiation Laboratory, Berkeley, 1957.
[6] H. Anger, Scintillation camera with multichannel collimators, J. Nucl. Med. 5 (1964) 515–531.
[7] R. Dreyer, R. Muenze, Labeling of human serum albumin with 99m-Tc (in German), Nat. Wiss. R. 18 (1969) 629–633.
[8] W.C. Eckelmann, Unparalleled contribution of technetium-99m to medicine over 5 decades, JACC (J. Am. Coll. Cardiol.): Cardiovasc. Imag. 2 (2009) 364–368.
[9] OECD Nuclear Energy Agency High-Level Group on the Security of Supply of Medical Radioisotopes, The Supply of Medical Radioisotopes - 2015 Medical Isotope Supply Review: ^{99}Mo/^{99m}Tc Market Demand and Production Capacity Projection 2015-2020, Nuclear Development NEA/SEN/HLGMR 5, OECD NEA, Paris, 2015.
[10] Yu Kotschkov, V.V. Pozdeyev, A.I. Krascheninnikov, N.V. Zakharov, Production of fission ^{99}Mo with closed uranium cycle at the nuclear reactor WWR-Ts (in Russian), Radiokhimiya 54 (2012) 173–177.
[11] A. Sameh, H.J. Ache, Production techniques for fission molybdenum-99, Radiochim. Acta 41 (1987) 65–72.
[12] L.C. Brown, Methods and Apparatus for Selective Gaseous Extraction of Molybdenum-99 and Other Fission Product Radioisotopes, 2015. Patent EP 2580763 B1.
[13] R. Muenze, O. Hladik, G. Bernhard, W. Boessert, R. Schwarzbach, Large scale production of fission ^{99}Mo by using fuel elements of a research reactor as starting material, Int. J. Appl. Radiat. Isot. 35 (1984) 49–54.
[14] D. Novotny, G. Wagner, Procedure of small scale production of Mo-99 on the basis of irradiated natural uranium metal as target, in: Consultants Meeting on Small Scale Production of Fission Mo-99 for Use in Tc-99m Generators, IAEA, Vienna, July 7–10, 2003.
[15] J. Sauerwein, K. Brooks, C. Critch, Selective gas extraction: a transformational production technology being implemented by GA, MURR and NORDION, in: Mo-99 Topical Meeting on Molybdenum-99 Technology Developments, Boston, MA, Aug. 31-Sept, vol. 3, 2015.
[16] G.J. Beyer, B. Eichler, T. Reetz, R. Muenze, J. Comor, New head process for non-HEU ^{99}Mo-production based on the oxidation of irradiated UO_2-pellets forming soluble U_3O_8, Nucl. Technol. Radiat. Prot. 31 (2016) 102–108.
[17] S.-K. Lee, G.J. Beyer, J.S. Lee, Development of industrial-scale fission ^{99}Mo production using low enriched uranium target, Nucl. Eng. Technol. 48 (2016) 613–623.
[18] H.J. Ryu, C.K. Kim, M. Sim, J.M. Park, J.H. Lee, Development of high-density U/Al dispersion plates for Mo-99 production using atomized uranium powder, Nucl. Eng. Technol. 45 (2013) 979–986.
[19] M. Druce, Australian's Experiences with Non-HEU Mo-99 Production, Supporting Small-Scale Non-HEU Mo-99 Production Capacity Building, Coordination Meeting for TC Project INT1056, IAEA, Vienna, 2013.
[20] G.F. Vandegrift, G. Hofman, C. Conner, J. Sedlet, D. Walker, A. Leonard, E.L. Wood, T.C. Wiencek, J.L. Snelgrove, A. Mutalib, B. Purwadi, H.G. Adang, L. Hotman, K. Moeridoen, A. Sukmana, A.S. Sriyono, H. Nasution, D.L. Amin, A. Basiran, A. Gogo, D. Sunaryadi, T. Taryo, Full-scale demonstration of the CINTICHEM process for the production of Mo-99 using a low-enriched target, RERTR Meeting, Sao Paolo, Brazil (1998). Oct. 18-23.
[21] G.F. Vandegrift, D. Stepinski, J. Jerden, A. Gelis, E. Krahn, L. Hafenrichter, J. Holland, GTRI Process Technology in Technical Development for Conversion of ^{99}Mo Production to Low Enriched Uranium, RERTR Meeting, Santiago, 2011. Chile Oct. 23-27.
[22] J. Kuperman, The global threat reduction initiative and conversion of isotope production to LEU targets, in: Paper Presented at the 2004 International Meeting on Reduced Enrichment for Research and Test Reactors, Vienna, October 7, 2004.
[23] A. Sameh, Production cycle for large scale fission Mo-99 separation by the processing of irradiated LEU uranium silicide fuel element targets, Sci. Technol. Nucl. Install. (2013) 704846.
[24] S. Dittrich, History and actual state of non-HEU fission-based Mo-99 production with low-performance research reactors, Sci. Technol. Nucl. Install. (2013) 514894.
[25] R. Muenze, G.J. Beyer, R. Ross, G. Wagner, D. Novotny, E. Franke, M. Jehangir, S. Pervez, A. Mushtaq, The fission-based ^{99}Mo production process ROMOL-99 and its application to PINSTECH Islamabad, Sci. Technol. Nucl. Install. (2013) 932546.
[26] T. Kim, S.-K. Lee, S. Lee, J.S. Lee, S.W. Kim, Development of silver nanoparticle–doped adsorbents for the separation and recovery of radioactive iodine from alkaline solutions, Appl. Radiat. Isot. 129 (2017) 215–221.
[27] W.D. Bond, W.E. Clark, Reduction of Cupric Oxide by Hydrogen. I. Fundamental Kinetics, ORNL-2815, Oak Ridge National Laboratory, Oak Ridge, 1960.
[28] T.W. Bowyer, R. Kephart, P.W. Eslinger, J.I. Friese, H.S. Mile, P.R. Saey, Maximum reasonable radioxenon releases from medical isotope production facilities and their effect on monitoring nuclear explosions, J. Environ. Radioact. 115 (2003) 192–200.
[29] International Atomic Energy Agency, Management of Radioactive Waste from “Mo Production, IAEA-TECDOC-1051, IAEA, Vienna, 1998.